UNIDIRECTIONAL SULFATE INGRESS IN LIMESTONE CALCINED CLAY CEMENT (LC^3) PASTES UNDER CYCLIC EXPOSURE

Qiao Wang* (1), William Wilson (1) and Karen Scrivener (1)

(1) École Polytechnique Fédérale de Lausanne, Switzerland

Abstract

If sulfate attack on Portland cement systems has been largely investigated in the last decades, mechanisms of sulfate resistance for systems with new SCMs are still in dim, especially for the emerging materials that are limestone calcined clay cements (LC^3). Using a new semi-immersion approach, we forced the penetration of sulfate ions in just one direction into LC^3 pastes under the capillary rise effect. To enhance the degradation process, highly concentrated sodium sulfate solution of 50 g/L and a cyclic exposure regime (20˚C & 78% RH followed by 40˚C & 33% RH) were employed in this paper. During exposure, lateral expansion was measured over time, showing almost negligible expansion for the LC^3 cement paste even after 56 days of very harsh exposure conditions. Simultaneously, microanalytical studies on the composition of hydration products were carried out by SEM-mapping to explain the expansion mechanisms. The results showed that the novel approach was adequate for cyclic exposure experiments, to investigate the full depth of degradation along the penetrating direction. Based on the analysis of BSE micrographs, phase distribution maps and expansion profiles, the gypsum and the ettringite were found to coexist in the voids resulting in a densified layer which could be associated with the most expansive zone. Overall, this study highlights the potential of the unidirectional semi-immersed method to link the sulfate attack expansion of cement pastes with the underlying mechanisms.

Keywords: LC^3; Sulfate attack; Unidirectional penetration; SEM; Degradation

1 INTRODUCTION

If concrete is considered as a durable construction material in most cases, durability problems may occur when concrete is exposed to deleterious ions, such as chloride and sulfate ions. Sulfate ions often invade inside to react with microstructure phases resulting in structure degradation, including expansion, cracking, spalling and eventually disintegration of concrete material. Even if many studies are available on the subject in literature, there are still open questions regarding this degradation process, such as the misleading nomenclature dividing sulfate attack into “chemical sulfate attack” and “physical sulfate attack”, the mechanisms of this “physical sulfate attack” being not well understood so far. As an example, previous studies

indicated that the gypsum can only precipitate in the already existed cracks which was the result of expansion but not the cause of it [1–3].

The most common conventional method to test the sulfate attack resistance is longitudinal expansion measurement of mortar bars in ponding test, but this approach only considers chemical sulfate attack. Another approach focussing on physical sulfate attack is the semi-immersion test in which a very complicated capillary flow which makes microstructure characterization not practical. Although those approaches were used in several studies (e.g., [4–6]), no obvious relationship was established between expansion and the amount of ettringite formed, which is perhaps due to the sulfate ions ingression in radial and longitudinal directions (eventually not only causing expansion in longitudinal direction). Therefore, the unidirectional test is presumably the most practical and effective approach to know the details along each parallel depth from the solution exposing surface[7,8].

In this paper, the main idea is to use the new established setup with LC³ cement paste exposed to a cyclic exposure regime. By this unidirectional approach, sulfate ions can only invade from bottom to top part under the capillary suction, enabling precise characterization of the structural alteration at different levels. The most competitive point of this investigation approach is that the same sample can be fully characterized over the full depth, i.e., expansion, phase distribution and pore structures. As demonstrated below, the results mainly show that coexistence of ettringite and gypsum in a densified layer in the microstructure causes expansion, in a layered degradation process.

2 MATERIALS AND EXPERIMENTAL APPROACHES

2.1 Materials

• *LC³-50 Cement*

The LC³-50 cement employed in this study was composed of 53 % Portland cement, 30 % calcined clay, 15 % limestone and 2 % gypsum. The chemical composition of Portland cement is displayed in

Table ***1***. A water to binder ratio of 0.6 was used to prepare cement pastes.

Table 1: Chemical composition of PC

Chemical composition (wt%)	SiO_2	Al_2O_3	Fe_2O_3	CaO	MgO	SO_3	Na_2O	K_2O	TiO_2	P_2O_5	LOI
Portland cement	20.4	5.1	1.9	64.2	1.0	2.9	0.4	0.7	0.2	0.2	1.67

• Sodium sulfate

Chemically analytical pure salt contains more than 99 % Na_2SO_4 solid was used as the external sulfate source. A solution of 50 g/L Na_2SO_4 was prepared for exposure of the specimen.

• Sample preparation

Cement pastes were mixed with water using metallic sector shape stirrer for 120 s with a speed of 1600 rpm. Then, they were casted in plastic cylinder containers with diameter of 33 mm, length of 60 mm. After one day, they were demoulded and cured in a slightly bigger container with only small amount of water to avoid leaching. The sample was cut into slices with thickness of 5 mm (both external surfaces with around 3 mm of the sample were removed). The

slices were then ready for installation in the semi-immersion setup, as illustrated in Fig. 1. The setup was place in a 40 ˚C room with relative humidity 33 % and, after one week, the setup was transferred into a 20 ˚C room with relative humidity 78 %. This 2-week cycle was repeated until the age of testing.

(a) (b)

Figure 1: The setup for unidirectional sulfate penetration test

2.2 SEM analyses

The paste samples were examined by scanning electron microscopy (SEM, FEI ESEM XL 30) using backscattered electrons and later on hyper mapping to get the elemental information of each pixel of maps. The elemental information from energy diffraction spectroscopy (EDS) is the foundation of this analysis. The Esprit 1.9 software was used to quantify the mapping data with the Hyper Map Mode after calibration with standards. After the calculation, the matrix of the points on the map of each element can be obtained, as well as the colorful maps of elemental distribution.

The magnification of elemental mappings was ×300, resolution was 1000×750 pixels, corresponding scanning area was about 860×645 μm, high voltage was 15.0 kV, and working distance was 12.5 mm. The images were then quantitatively analyzed using the EDXIA approach developed by F. Georget[9].

2.3 Expansion measurements

The lateral expansion was measured parallel to the degradation front (parallel to the exposed surface). The measurement was carried out as shown in Fig. 2, using 1-mm thick steel rings and a digital slide calliper.

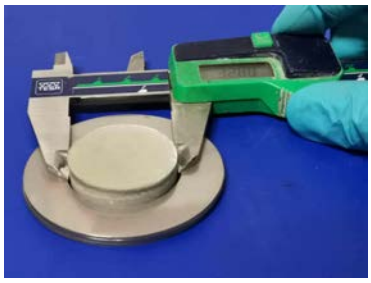

Figure 2: Lateral expansion measurement

3 RESULTS AND DISCUSSION

3.1 Visual inspection

Fig. 3 shows the LC³ cement samples appearance after exposure to sulfate solution. At 28d, samples were intact without any visual damage. At 56d, it was more degraded because the samples were fully penetrated by sulfate ions from bottom to top portion under the flow of capillary rise. The white deposits on the top surface indicates penetration over the full depth of the sample. Because the bottom was directly exposed to the solution, small cracks appeared with longer time of exposure and degradation.

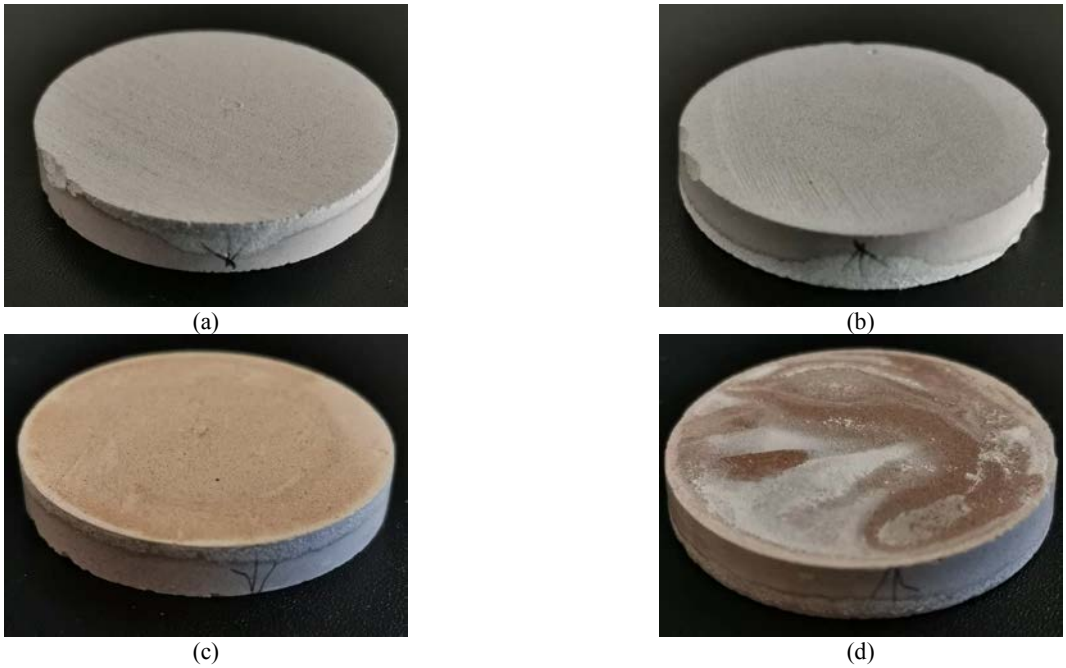

Figure 3: Visual observations of LC³ samples showing (a) bottom surface of 28d sample, (b) top surface of 28d sample, (c) bottom surface of 56d sample, (d) top surface of 56d sample

3.1.1 Expansion vs. depth

The evolution of expansion profiles along the sulfate ions penetrating direction was tracked with time, as shown in Fig. 4. Shrinkage occurred from the top of the LC³ sample with very good resistance to expansion. After 56d of exposure, a slight expansion was measured with a peak at around 0.5 mm. It is of interest to understand why a higher expansion occurred at this point. The comparison with a Portland cement system (PC) in less harsh exposure conditions (w/c=0.6, 30 g/L concentration, constant RH 55 %) shows how the expansion at 28d was much higher than LC³ samples at all ages. It is also interesting to note that the most expanded layers of PC were deeper than LC³ at the same age which illustrates how LC³ system can be more resistant to invading sulfate ions.

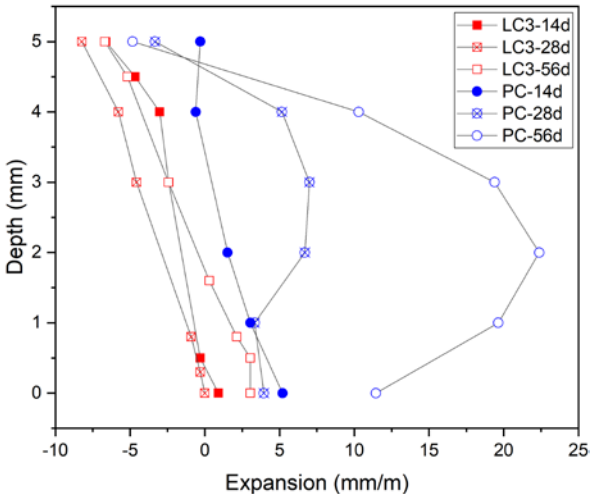

Figure 4: Expansion profile for LC³ cement paste at different ages, in comparison with a PC paste exposed to less harsh conditions [7]

3.1.2 Qualitative analysis of BSE images

When the significant changes according with the expansion are seen, it must be something happening in the microstructure. From a qualitative analysis of BSE images, the porosity variation over depth can be clearly seen in Fig. 5. At 28d of exposure, a bottom layer of approximately 0.5 mm was densified due to the new hydrates precipitating in the cement paste voids. With time, the densified front shifted deeper towards the top of the sample and a porous degraded layer remained below, as seen from the visual evidence at 56d. It is exactly the reason that the sulfate ions can still move inside easily in such a porous material. In later age sample, cracks were observed in most cases parallel to external surface, but it is not clear if cracking occurred from the degradation or during sample preparation, as the cracks were empty at 56d.

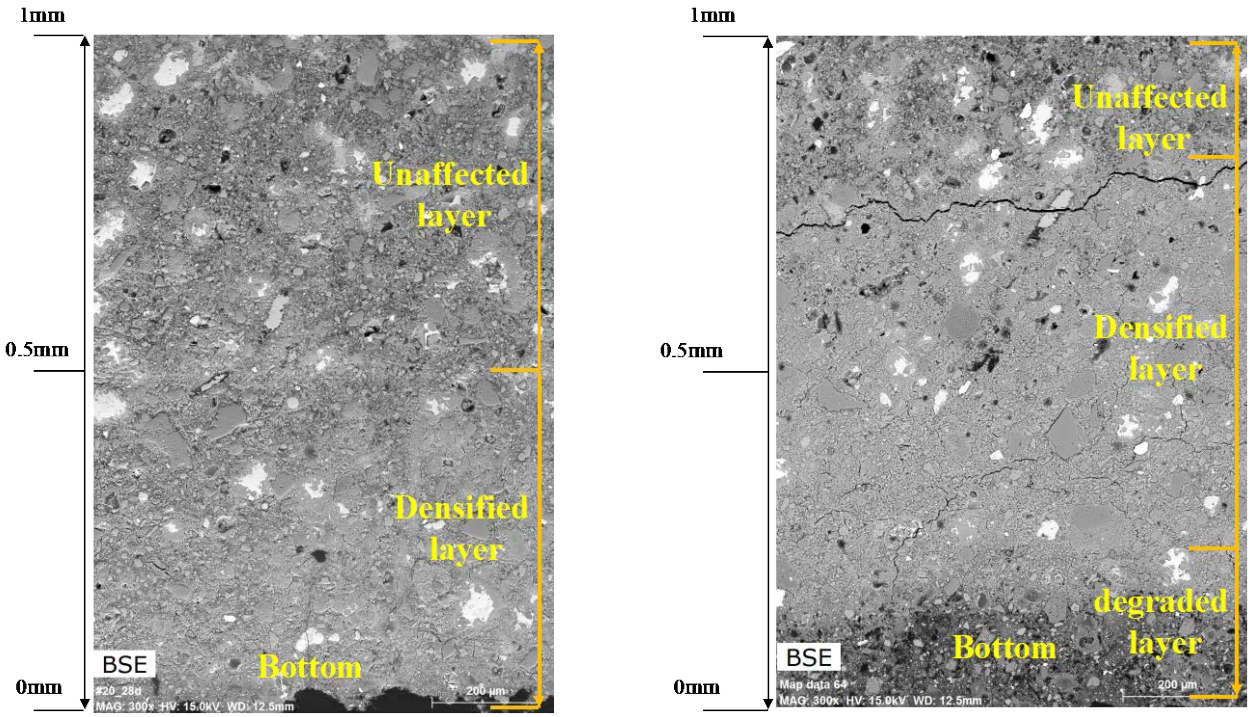

(a) (b)

Figure 5: Comparison of BSE imaging of the bottom of LC³ samples after exposures of (a) 28d and (b) 56d

From a large-scale picture in Fig. 6, the degraded LC³ cement sample consists of three obvious different zones. A fully degraded zone with many pores was noticed in subsurface. Second layer was densified and this region had the highest expansion propagation in contrast with expansion evolution curve. The third layer was the unaffected area and it was a normal porous cement paste matrix. It can be seen that the sulfate attack is a layered-damage process, and the main internal damaging stress was from the crystals growing in the small voids[10,11].

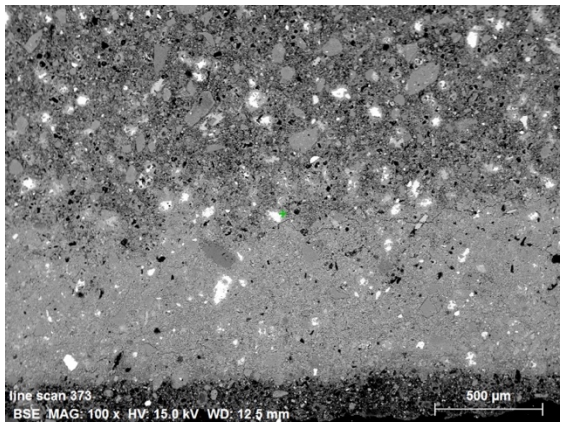

Figure 6: Low-magnification micrography of the bottom part after 56-day exposure

3.2 Quantitative results from SEM-EDS analysis

3.2.1 Phase maps

The phase maps were obtained from the SEM-EDS mappings analysed using the EDXIA framework[9]. Fig. 7 presents phase maps overlaid on BSE micrographs, showing that the gypsum and ettringite hydrates were mainly precipitated in the densified areas. This result further supports that these two phases could cause expansion especially when they coexist[6]. AFm and portlandite phases are the main phases consumed for the formation of ettringite and gypsum, which can be observed from the 56d map. Furthermore, the first 200 micrometres were totally degraded with high porosity at 56d. Above the densified layer, more portlandite and AFm phases were present. However, it was quite difficult to detect the ettringite phase since they were precipitated in very small pores mixed with C-S-H phase, at a scale smaller than the interaction volumes investigated by SEM-EDS.

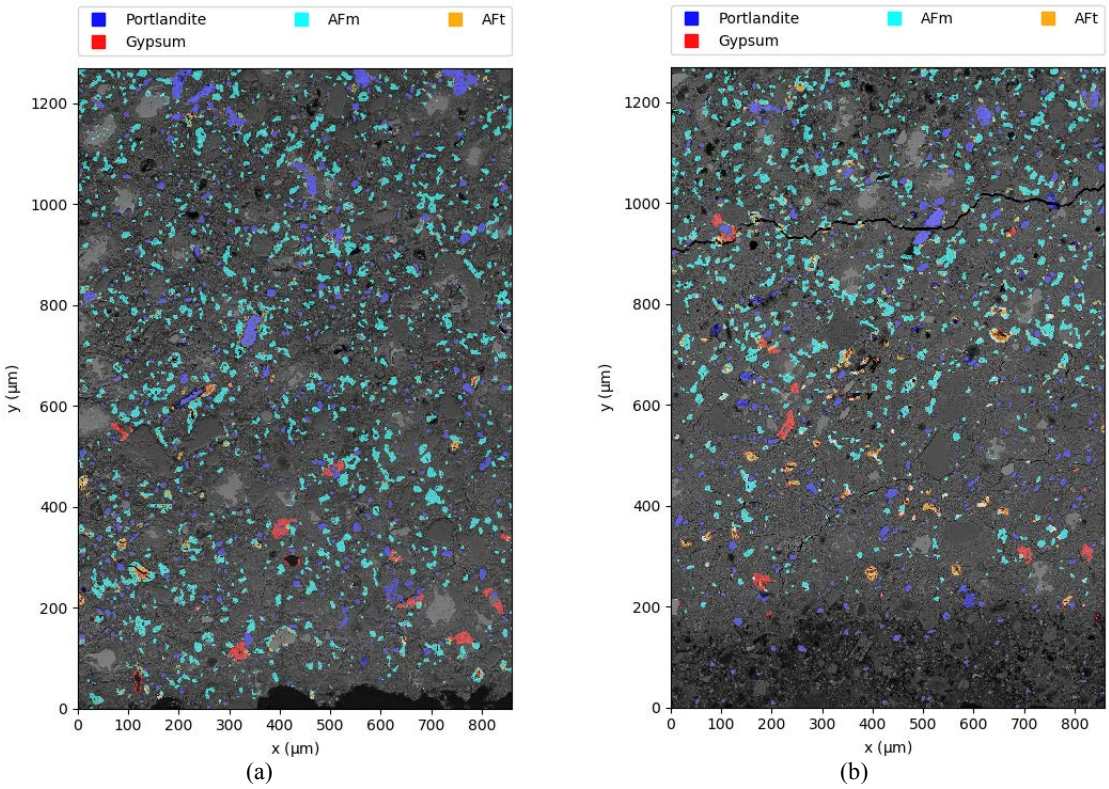

Figure 7: Phase composition maps of LC^3 cement at 28d & 56d. (a) 28d; (b) 56d

3.2.2 Phase profile

The profiles along the depth are displayed for the phases of interest in Fig. 8. It can be visually seen that the gypsum-rich front position can be well correlated with the expansion profile. According to Fig. 8, AFm and Portlandite can be tracked to verify which area is still

intact (the amount of these phases is likely to be higher compared with degraded zones). Therefore, the front of AFm and Portlandite can be used for the estimation of depth of degradation. But there is still one thing missing, ettringite.

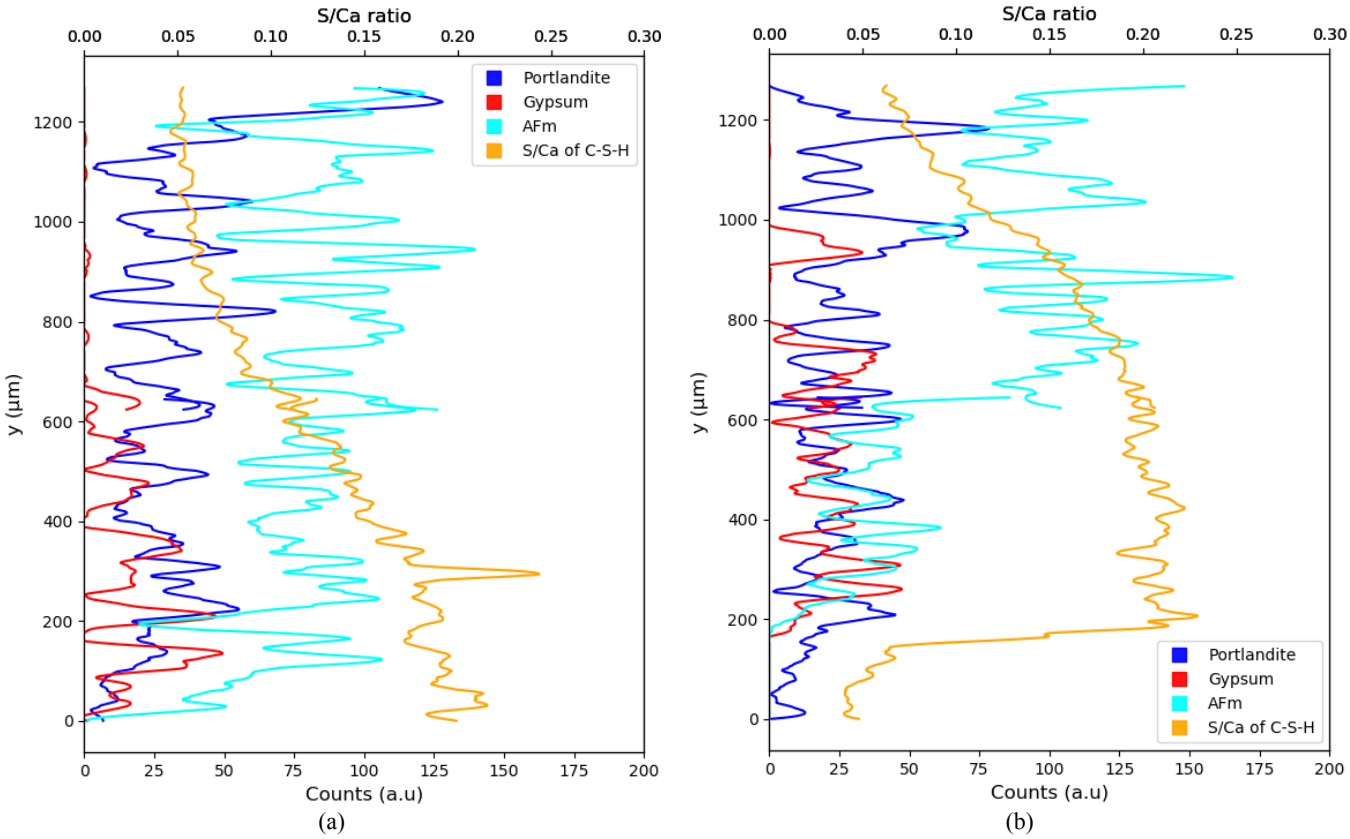

Figure 8: Phase and S/Ca profiles of LC³ pastes exposed to sulfate solution for (a) 28d and (b) 56d.

However, sub-micron sized ettringite presence can be indirectly determined with the profile of atomic ratios of the C-S-H phase. The profile of S/Ca ratio was plotted in Fig. 8 and it proved to enable the identification of ettringite-rich zones of C-S-H. For example, at 56d, the hump from 200 to 800 µm with higher S/Ca value (S/Ca=0.5 for ettringite) than the rest which implies that ettringite was probably intermixed with C-S-H phase. Ettringite precipitated in the shallow depth at 28d and it moved deeper at 56d. The comparison with phase maps, BSE micrographs and expansion measurements showed that a densified layer with coexisting ettringite and gypsum is present, although it does not lead to significant expansion during the length of the test.

4 CONCLUSIONS

This study showed the potential of using a unidirectional semi-immersion approach to simultaneously investigate the expansion and the microstructure degradation due to the chemical sulfate attack in a LC³-50 system. The main findings are the following:

- The novel unidirectional semi-immersion approach was adapted to harsh cycling exposure conditions and provided insights on sulfate attack mechanisms in LC³ systems;
- LC³ cement paste showed a good resistance to sulfate attack even in an aggressive environment (cyclic exposure & high solution concentration), showing slow ingress of sulfate ions and slight expansion;
- The results showed that the sulfate attack is a layered-damage process: a densified layer with coexisting ettringite and gypsum penetrates progressively trough the cement paste, potentially leading to expansion.

Overall, this short study showed the microstructure damage near the surface exposed to the sulfate solution, but further work will focus on investigating the salt crystallization mechanisms which are likely taking place at near the surface of the sample exposed to air, due to the evaporation and the reprecipitation of sodium sulfate salts.

REFERENCES

[1] T. Schmidt, B. Lothenbach, M. Romer, J. Neuenschwander, K. Scrivener, Physical and microstructural aspects of sulfate attack on ordinary and limestone blended Portland cements, Cem. Concr. Res. 39 (2009) 1111–1121.

[2] R.S. Gollop, H.F.W. Taylor, Microstructural and microanalytical studies of sulfate attack. I. Ordinary portland cement paste, Cem. Concr. Res. 22 (1992) 1027–1038.

[3] C. Yu, W. Sun, K. Scrivener, Mechanism of expansion of mortars immersed in sodium sulfate solutions, Cem. Concr. Res. 43 (2013) 105–111.

[4] A.R.S. M.L. Nehdi, A.M. Soliman, Investigation of concrete exposed to dual sulfate attack, Cem. Concr. Res. 64 (2014) 42–53.

[5] Z. Shi, S. Ferreiro, B. Lothenbach, M.R. Geiker, W. Kunther, J. Kaufmann, D. Herfort, J. Skibsted, Sulfate resistance of calcined clay – Limestone – Portland cements, Cem. Concr. Res.116 (2019) 238–251.

[6] W. Kunther, Investigation of Sulfate Attack by Experimental and Thermodynamic Means, PhD Thesis, EPFL, 2012.

[7] Qiao Wang, William Wilson, Karen Scrivener, Unidirectional penetration approach for characterizing dual sulfate attack mechanisms on cementitious materials, (In preparation).

[8] W. Qiao, W. William, S. Karen, Investigating dual sulfate attack mechanisms using unidirectional penetration approach, in: Toulouse, France, 2020.

[9] F. Georget, W. Wilson, K. Scrivener, Comprehensive microstructure phase characterization from quantified SEM-EDS maps in cementitious materials (In preparation)

[10] S. Siegesmund, R. Snethlage, eds., Stone in Architecture: Properties, Durability, 5th ed., Springer-Verlag, Berlin Heidelberg, 2014.

[11] E.M. Winkler, P.C. Singer, Crystallization Pressure of Salts in Stone and Concrete, GSA Bull. 83 (1972) 3509–3514.